

Refractive index sensing using ultrasonically crushed polymer optical fibers

Shumpei Shimada¹, Heeyoung Lee¹, Makoto Shizuka¹, Hiroki Tanaka¹, Neisei Hayashi², Yukihiro Matsumoto³, Yosuke Tanaka⁴, Hitoshi Nakamura⁵, Yosuke Mizuno^{1*}, and Kentaro Nakamura¹

¹Institute of Innovative Research, Tokyo Institute of Technology, Yokohama 226-8503, Japan

²Research Center for Advanced Science and Technology, The University of Tokyo, Meguro, Tokyo 153-8904, Japan

³Department of Architecture and Civil Engineering, Toyohashi University of Technology, Toyohashi, Aichi 441-8580, Japan

⁴Institute of Engineering, Tokyo University of Agriculture and Technology, Koganei, Tokyo 184-8588, Japan

⁵Department of Civil and Environmental Engineering, Tokyo Metropolitan University, Hachioji, Tokyo 192-0397, Japan

*E-mail: ymizuno@sonic.pi.titech.ac.jp

Received October 26, 2016; accepted November 7, 2016; published online November 24, 2016

We demonstrate power-based refractive index (RI) sensing using an ultrasonically crushed polymer optical fiber (POF). This structure can be easily and cost-effectively fabricated within a short time (i.e., ~ 1 s) without the need to employ external heat sources or chemicals. The only requirement is to simply press a horn connected to an ultrasonic transducer against part of the POF. The RI dependence of the transmitted power shows linear trends in RI ranges of ~ 1.32 to ~ 1.36 [coefficient: -62 dB/RIU (RI unit)] and ~ 1.40 to ~ 1.44 (coefficient: -257 dB/RIU). The temperature dependence of the transmitted power is also investigated. © 2017 The Japan Society of Applied Physics

Optical fiber sensors have been vigorously studied because of their ability to measure various physical parameters, such as strain,^{1,2)} temperature,^{1,2)} pressure,³⁾ acoustic impedance,^{4,5)} humidity,⁶⁾ reflectivity,^{7,8)} and nuclear radiation.⁹⁾ Among these applications, refractive index (RI) sensing using optical fibers has been attracting considerable attention in biological and chemical research. Furthermore, numerous techniques have been developed in the past several decades.^{10–13)} RI sensing based on evanescent waves generated in the tapered region of glass optical fibers^{12,13)} is one of the most cost-effective techniques having high sensitivity. However, glass optical fiber tapers are fragile and need to be fabricated and handled with care. One promising way to address this concern is to exploit polymer optical fiber (POF) tapers,^{14–20)} which exhibit much greater flexibility.

Various POF tapering methods have been developed to date. Two widely used methods are based on a heat-and-pull technique with an external heat source^{14–17)} and a chemical etching technique.¹⁸⁾ However, employing external heat sources (e.g., flame,¹⁴⁾ compact furnaces,^{15,16)} or a solder gun¹⁷⁾ and chemicals is unsafe and inconvenient. A POF tapering technique for converting the propagating light energy into heat without using an external heat source has been developed.¹⁹⁾ However, the required high-power light injection may cause burning at the POF ends²¹⁾ and/or what is called the fuse effect.^{22,23)} RI sensing using V-shaped POFs has also been reported.²⁰⁾ However, their measurement accuracy is not sufficiently high because of their structural instability.

To the best of our knowledge, this is the first work to demonstrate RI sensing using an ultrasonically crushed POF. This structure can be easily fabricated without the need to employ external heat sources or chemicals. A horn connected to an ultrasonic transducer is pressed against part of the POF for only a short period. First, we clarify that the RI dependence of the transmitted power shows nonmonotonic behavior, which indicates that this RI sensor can be directly used only in limited RI ranges. For instance, the dependence coefficients are -62 dB/RIU (RI unit) and -257 dB/RIU in RI ranges of ~ 1.32 to ~ 1.36 and ~ 1.40 to ~ 1.44 , respectively. We then find that the transmitted power shows a negative dependence on temperature with a coefficient of -0.094 dB/ $^{\circ}$ C when the RI is fixed at 1.33, thereby leading to the feasibility of temperature compensation in RI sensing.

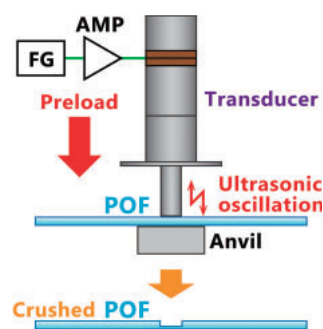


Fig. 1. Processing procedure for the partially crushed polymer optical fiber. FG: function generator.

The POF used in the experiment was a perfluorinated graded-index (PFGI) POF^{24,25)} with a core diameter of $50\ \mu\text{m}$, a cladding diameter of $70\ \mu\text{m}$, an overcladding diameter of $490\ \mu\text{m}$, and a propagation loss of ~ 250 dB/km at 1550 nm. The RIs of the core center, cladding, and overcladding at 1550 nm were 1.356, 1.348, and 1.590, respectively. The core and cladding layers consisted of identical material [i.e., poly(perfluorobutenylvinyl) ether with different dopant concentrations]. Their boundary was not visible. In contrast, the overcladding layer was composed of polycarbonate. Its boundary with the cladding layer was observable with a microscope. PFGI-POFs are known to absorb much less water than the standard poly(methyl methacrylate)-based POFs,^{14,16)} which is desirable for liquid RI sensing.²⁶⁾

Figure 1 illustrates the POF processing procedure. A horn (diameter: $6\ \text{mm}$) connected to a Langevin-type ultrasonic transducer with a resonance frequency of ~ 18.7 kHz was pressed for 1 s against the midpoint of the 40 -cm-long POF on an anvil (made of stainless steel) with a $10\ \text{N}$ preload.²⁷⁾ Note that the output voltage from a function generator was amplified and applied to the piezoelectric stack of the transducer. The vibration velocity was measured by Doppler velocimetry to be $2.3\ \text{m/s}$. A 6 -mm-long region of the POF was then crushed. The POF was first partially melted using this ultrasonic method and then solidified after distortion. The processes resulted in stable fabrication. Stable fabrication of the crushed structure was difficult because simple pressing without ultrasonic oscillations was susceptible to incomplete plastic

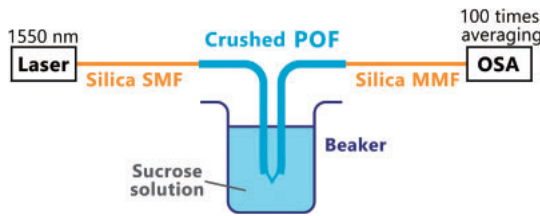


Fig. 2. Experimental setup for RI sensing using the crushed POF. MMF: multimode fiber, OSA: optical spectrum analyzer, and SMF: single-mode fiber.

deformation. The crushed region was bent around its midpoint for ease of handling. It was also used as a sensing head.

Figure 2 shows an experimental setup for RI sensing using the crushed POF. The output light from a laser at 1550 nm (power: 10 dBm; bandwidth: ~1 MHz) was guided through a 1-m-long silica single-mode fiber (SMF) and injected into the POF. The transmitted light was then guided to an optical spectrum analyzer (OSA) via a 3-m-long silica multimode fiber with a core diameter of 50 μm to suppress the optical coupling loss at the boundary between the POF and the silica fiber. Its spectral peak power was precisely measured using 100× averaging. Both POF ends were connected to the silica fibers by butt-coupling via ferrule connector/subscriber connector adaptors.²⁵⁾

We first investigated the RI dependence of the transmitted power when the crushed region was immersed in a sucrose solution at 25 °C, the RI of which was varied from 1.318 to 1.437 by controlling the concentration in the range from 0 to 65%.²⁸⁾ Subsequently, the temperature dependence of the transmitted power was investigated in the range from 10 to 35 °C when the ambient RI of the crushed region was fixed at 1.333 (concentration: 10%).

Figures 3(a)–3(d) show micrographs of the crushed POF. Figures 3(a) and 3(b) present side views around the boundary between the crushed and uncrushed regions and around the middle of the crushed region, respectively. The crushed region had a height of ~270 μm, which was ~1.8 times smaller than the outer diameter (490 μm) of the uncrushed region. Figures 3(c) and 3(d) show top views around the boundary and around the midpoint, respectively. The width of the crushed region was ~850 μm, which was ~1.7 times larger than the initial outer diameter (490 μm). Figure 3(e) presents a photograph of the crushed POF after bending. The bending angle around the midpoint of the crushed region was ~35°.

Figure 4(a) shows the measured RI dependence of the transmitted power at 25 °C. The vertical axis was normalized such that the power at RI = 1.318 (sucrose concentration = 0%) became 0 dB. Note that the propagation loss in the crushed region of the POF was ~35 dB. The transmitted power decreased, and the loss increased as the RI increased to ~1.36. However, it increased by ~1 dB when the RI increased to ~1.37. Subsequently, the power decreased monotonically with increasing RI. The dependence abruptly became large when the RI was higher than ~1.40. When the RI was 1.333, 1.384, and 1.437, the measurement errors, defined as the standard deviations of the power fluctuations (the power was measured every 1 min for 1 h) were ±0.30, 0.42, and 0.63 dB, respectively. This nonmonotonic behavior seems to originate in part from a change in the phase mismatching condition among the modes involved in the

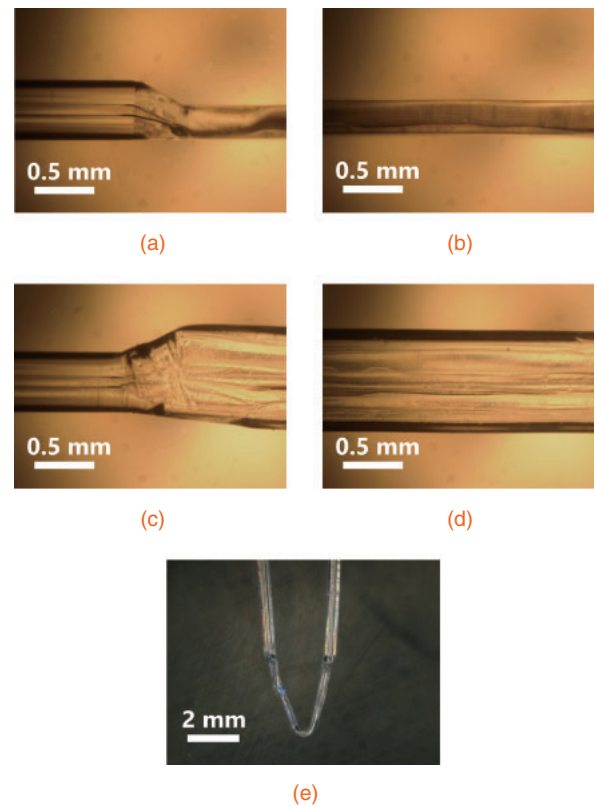


Fig. 3. Micrographs of the crushed polymer optical fiber: (a, b) side views and (c, d) top views; (a, c) around the boundary between the crushed and uncrushed regions and (b, d) around the middle of the crushed region; and (e) photograph of the crushed region bent around its midpoint.

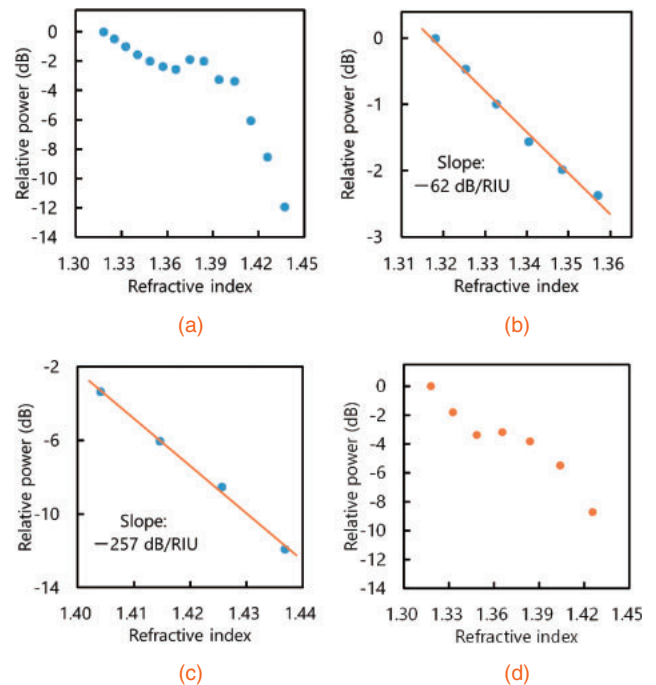


Fig. 4. Measured relative transmitted power dependence on the RI. Panels (b) and (c) show magnified views of (a); (d) is the same measurement result as (a) when an independently fabricated crushed POF was used. The RI ranges are (a, d) 1.318–1.437, (b) 1.318–1.357, and (c) 1.404–1.437.

process when the external RI is varied, as observed in tapered silica SMF.²⁹⁾ The situation should be more complicated, not only because of the multimodal nature of the POF

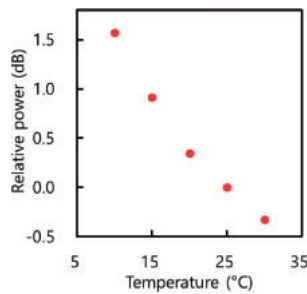


Fig. 5. Relative transmitted power dependence on temperature when the RI was fixed at 1.333.

but also because of the non-axisymmetrical structure of the crushed POF. The transmitted power and the RI were not in one-to-one correspondence with each other. Hence, the RI range needed to be limited for practical sensor application. The transmitted power directly provided the RI value with a dependence coefficient of -62 dB/RIU if the RI range was limited to ~ 1.32 to ~ 1.36 [Fig. 4(b), magnified view of this RI range]. In the same manner, the transmitted power corresponded with the RI with a dependence coefficient of -257 dB/RIU if the RI range was limited to ~ 1.40 to ~ 1.44 [Fig. 4(c)]. Fairly comparing these absolute values with those in previous reports measured under different conditions and POF structures was difficult. However, the negative coefficient of the transmitted power (or the positive coefficient of the loss) against the RI agreed with some of the previous POF-taper-based results.^{14,19} No quantifiable influence on the transmitted power was observed when the uncrushed regions of the POF were immersed in the sucrose solutions. Note that this nonmonotonic behavior was reproduced to some extent when we used an independently fabricated crushed POF [see Fig. 4(d)], showing a higher repeatability than other POF-based techniques we have reported;^{19,20} further investigation of this point is required.

We finally set the ambient RI of the crushed region to 1.333 (sucrose concentration: 10%), which was located near the midpoint of the linear region shown in Fig. 4(b). We then investigated the temperature dependence of the transmitted power in the range from 10 to 35 °C. The vertical axis was normalized so that the power measured at 25 °C became 0 dB. The influence of the temperature dependence of the sucrose solution was compensated.³⁰ The transmitted power decreased monotonically with increasing temperature (Fig. 5). This behavior was the same as that of the bent-POF-based sensors.³¹ The temperature dependence coefficient of the transmitted power was -0.094 dB/°C when we applied a roughly linear fit to the data in this range. The temperature-dependent error in RI sensing can be compensated in principle once this one-to-one correspondence between the RI and the temperature is known.

In conclusion, we demonstrated RI sensing by exploiting an ultrasonically crushed POF, the structure of which can be easily fabricated without the need to employ external heat sources or chemicals. The only requirement is to simply press a horn connected to an ultrasonic transducer against part of the POF for a short time (e.g., ~ 1 s). The transmitted power was first experimentally shown to have a nonmonotonic dependence on the RI with moderate repeatability. This observation indicated that using this sensor directly in the

entire RI range was difficult. However, the transmitted power and RI in limited RI ranges were in a one-to-one correspondence with dependence coefficients of -62 dB/RIU (RI from ~ 1.32 to ~ 1.36) and -257 dB/RIU (RI from ~ 1.40 to ~ 1.44). A negative dependence of the transmitted power on the temperature (coefficient: -0.094 dB/°C) was also clarified when the RI was fixed at 1.33, which leads to the possibility of temperature compensation in RI sensing. Thus, we anticipate that this unique RI sensing based on the ultrasonically crushed POF will be of great use in implementing stable and cost-effective fiber-optic RI sensors for future biological and chemical applications.

Acknowledgments This work was supported by the MLIT Construction Technology Research and Development Subsidy Program; by JSPS KAKENHI Grant Numbers 25709032, 26630180, and 25007652; and by research grants from the Japan Gas Association, the ESPEC Foundation for Global Environment Research and Technology, and the Association for Disaster Prevention Research.

- 1) Y. Mizuno, N. Hayashi, H. Fukuda, K. Y. Song, and K. Nakamura, *Light: Sci. Appl.* **5**, e16184 (2016).
- 2) Y. Dong, H. Zhang, L. Chen, and X. Bao, *Appl. Opt.* **51**, 1229 (2012).
- 3) J. Ma, W. Jin, H. L. Ho, and J. Y. Dai, *Opt. Lett.* **37**, 2493 (2012).
- 4) Y. Antman, A. Clain, Y. London, and A. Zadok, *Optica* **3**, 510 (2016).
- 5) N. Hayashi, H. Lee, Y. Mizuno, and K. Nakamura, *IEEE Photonics J.* **8**, 7100707 (2016).
- 6) G. Woyessa, K. Nielsen, A. Stefani, C. Markos, and O. Bang, *Opt. Express* **24**, 1206 (2016).
- 7) M. Shizuka, N. Hayashi, Y. Mizuno, and K. Nakamura, *Appl. Opt.* **55**, 3925 (2016).
- 8) T. Okamoto, D. Iida, K. Toge, and T. Manabe, *J. Lightwave Technol.* **34**, 4259 (2016).
- 9) P. Stajanca, L. Mihai, D. Sporea, D. Negut, H. Sturm, M. Schukar, and K. Krebber, *Opt. Mater.* **58**, 226 (2016).
- 10) H. J. Patrick, A. D. Kersey, and F. Bucholtz, *J. Lightwave Technol.* **16**, 1606 (1998).
- 11) T. Takeo and H. Hattori, *Jpn. J. Appl. Phys.* **21**, 1509 (1982).
- 12) Z. Tian, S. S. H. Yam, J. Barnes, W. Bock, P. Greig, J. M. Fraser, H. Loock, and R. D. Oleschuk, *IEEE Photonics Technol. Lett.* **20**, 626 (2008).
- 13) A. Leung, K. Rijal, P. M. Shankar, and R. Mutharasan, *Biosens. Bioelectron.* **21**, 2202 (2006).
- 14) D.-J. Feng, G.-X. Liu, X.-L. Liu, M.-S. Jiang, and Q.-M. Sui, *Appl. Opt.* **53**, 2007 (2014).
- 15) N. Hayashi, H. Fukuda, Y. Mizuno, and K. Nakamura, *J. Appl. Phys.* **115**, 173108 (2014).
- 16) Y. Jeong, S. Bae, and K. Oh, *Curr. Appl. Phys.* **9**, e273 (2009).
- 17) A. A. Jasim, N. Hayashi, S. W. Harun, H. Ahmad, R. Penny, Y. Mizuno, and K. Nakamura, *Sens. Actuators A* **219**, 94 (2014).
- 18) Y. M. Wong, P. J. Scully, H. J. Kadim, V. Alexiou, and R. J. Bartlett, *J. Opt. A* **5**, S51 (2003).
- 19) H. Ujihara, N. Hayashi, K. Minakawa, M. Tabaru, Y. Mizuno, and K. Nakamura, *Appl. Phys. Express* **8**, 072501 (2015).
- 20) H. Lee, N. Hayashi, Y. Mizuno, and K. Nakamura, *Jpn. J. Appl. Phys.* **54**, 118001 (2015).
- 21) Y. Mizuno, N. Hayashi, and K. Nakamura, *Opt. Lett.* **38**, 1467 (2013).
- 22) Y. Mizuno, N. Hayashi, H. Tanaka, K. Nakamura, and S. Todoroki, *Appl. Phys. Lett.* **104**, 043302 (2014).
- 23) Y. Mizuno, N. Hayashi, H. Tanaka, and K. Nakamura, *IEEE Photonics J.* **6**, 6600307 (2014).
- 24) Y. Koike and M. Asai, *NPG Asia Mater.* **1**, 22 (2009).
- 25) Y. Mizuno and K. Nakamura, *Appl. Phys. Lett.* **97**, 021103 (2010).
- 26) S. Ando, T. Matsuura, and S. Sasaki, *Chemtech* **24**, 20 (1994).
- 27) S. Shimada, H. Tanaka, K. Hasebe, N. Hayashi, Y. Ochi, T. Matsui, I. Nishizaki, Y. Matsumoto, Y. Tanaka, H. Nakamura, Y. Mizuno, and K. Nakamura, *Electron. Lett.* **52**, 1472 (2016).
- 28) D. R. Lide, *Handbook of Chemistry and Physics* (CRC Press, Boca Raton, FL, 2004).
- 29) S. Lacroix, R. J. Black, C. Veilleux, and J. Lapierre, *Appl. Opt.* **25**, 2468 (1986).
- 30) P. Schiebener, J. Straub, J. M. H. Levelt Sengers, and J. S. Gallagher, *J. Phys. Chem. Ref. Data* **19**, 677 (1990).
- 31) N. Jing, C. X. Teng, X. W. Zhao, and J. Zheng, *Appl. Opt.* **54**, 1890 (2015).